ANTIMICROBIAL AGENTS AND CHEMOTHERAPY, June 2010, p. 2480–2488 Vol. 54, No. 6
0066-4804/10/$12.00 doi:10.1128/AAC.00281-10

A Nonazole CYP51 Inhibitor Cures Chagas' Disease in a Mouse Model of Acute Infection▽†

Patricia S. Doyle,[1] Chiung-Kuang Chen,[2] Jonathan B. Johnston,[2] Stephanie D. Hopkins,[1] Siegfried S. F. Leung,[2] Matthew P. Jacobson,[2] Juan C. Engel,[1] James H. McKerrow,[1] and Larissa M. Podust[2]*

Sandler Center for Basic Research in Parasitic Diseases[1] and Department of Pharmaceutical Chemistry,[2] University of California, San Francisco, California 94158

Received 26 February 2010/Returned for modification 29 March 2010/Accepted 6 April 2010

Chagas' disease, the leading cause of heart failure in Latin America, is caused by the kinetoplastid protozoan *Trypanosoma cruzi*. The sterols of *T. cruzi* resemble those of fungi, both in composition and in biosynthesis. Azole inhibitors of sterol 14α-demethylase (CYP51) successfully treat fungal infections in humans, and efforts to adapt the success of antifungal azoles posaconazole and ravuconazole as second-use agents for Chagas' disease are under way. However, to address concerns about the use of azoles for Chagas' disease, including drug resistance and cost, the rational design of nonazole CYP51 inhibitors can provide promising alternative drug chemotypes. We report the curative effect of the nonazole CYP51 inhibitor LP10 in an acute mouse model of *T. cruzi* infection. Mice treated with an oral dose of 40 mg LP10/kg of body weight twice a day (BID) for 30 days, initiated 24 h postinfection, showed no signs of acute disease and had histologically normal tissues after 6 months. A very stringent test of cure showed that 4/5 mice had negative PCR results for *T. cruzi*, and parasites were amplified by hemoculture in only two treated mice. These results compare favorably with those reported for posaconazole. Electron microscopy and gas chromatography-mass spectrometry (GC-MS) analysis of sterol composition confirmed that treatment with LP10 blocked the 14α-demethylation step and induced breakdown of parasite cell membranes, culminating in severe ultrastructural and morphological alterations and death of the clinically relevant amastigote stage of the parasite.

Chagas' disease, caused by the kinetoplastid protozoan *Trypanosoma cruzi*, is the leading cause of heart failure in Latin America. The disease is transmitted naturally by hematophagous reduviid insects (6), but human infection may also occur via other routes, including blood transfusion, congenital infection, breast-feeding, organ transplant from chagasic donors, laboratory accidents, and ingestion of contaminated foods and beverages. The acute phase of infection usually occurs in children, and 5 to 10% of symptomatic patients may die. Following a subclinical "indeterminate" phase, a chronic phase involving heart failure and gastrointestinal tract lesions often ensues (37, 42). The only clinically available drugs for Chagas' disease are nifurtimox and benznidazole, both of which have been in use for 4 decades. While they have significant efficacy in the acute phase, both drugs suffer from the twin liabilities of serious side effects and low efficacy in the chronic phase. New drugs with improved efficacy and less toxicity are needed (14, 29).

The biosynthesis of membrane sterols is one of the metabolic pathways successfully targeted in the treatment of diseases caused by pathogenic fungi (48). Clinically employed antifungal azoles target sterol 14α-demethylase (CYP51), a cytochrome P450 enzyme that catalyzes oxidative removal of the 14α-methyl group of a sterol precursor to result in $\Delta^{14,15}$-desaturated intermediates in ergosterol biosynthesis (19, 20). Close similarities to fungi in sterol composition and biosynthesis, plus an absolute requirement for specific 24-methyl sterols for cell viability and proliferation, provide a basis for development of chemotherapy targeting the sterol biosynthetic pathway in *T. cruzi*. The successful application of antifungal drugs to anti-chagasic therapy exploits these similarities (38). In addition to compounds optimized for antifungal therapy, other CYP51 inhibitors with strong anti-*T. cruzi* activity have been reported (3, 8, 24, 44, 45).

Inhibitors of CYP51 are in the pipeline for preclinical and clinical development for treatment of Chagas' disease (11). Although earlier commercially available inhibitors, like ketoconazole and itraconazole, were not powerful enough to eradicate *T. cruzi* from infected animals or human patients (28), the recently approved inhibitor posaconazole (Noxafil; Schering-Plough) is capable of inducing parasitological cure in murine models of both acute and chronic Chagas' disease (18). Posaconazole cured 50 to 100% of animals in the acute phase and 50 to 60% of chronically infected animals (2). Very recently, posaconazole cured an immunosuppressed patient with concomitant Chagas' disease and systemic lupus erythematosus (34). However, the use of posaconazole as an anti-chagasic agent may be limited by the requirement for simultaneous intake of a fatty meal or a nutritional supplement to enhance absorption, the drug's high cost, and the need for clinical monitoring during treatment (31). Another complication is the rapid appearance of laboratory-induced resistance to azoles in *T. cruzi*, which may predict the occurrence of drug resistance in chagasic patients (4). Although no data on the development of posaconazole resistance in patients with Chagas' disease are

* Corresponding author. Mailing address: Department of Pharmaceutical Chemistry, University of California, San Francisco, CA 54158. Phone and fax: (415) 502-4728. E-mail: larissa.podust@ucsf.edu.

† Supplemental material for this article may be found at http://aac.asm.org/.

▽ Published ahead of print on 12 April 2010.

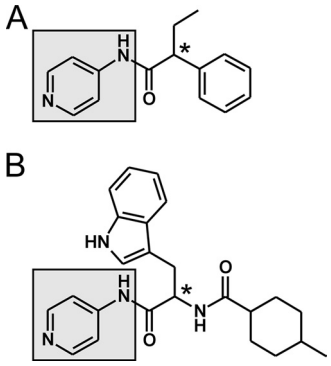

FIG. 1. Screen hit (A) and the expanded-spectrum compound LP10 (B) containing the *N*-[4-pyridyl]-formamide scaffold (highlighted in gray), which unvaryingly binds in the CYP51 active site. The chiral center is labeled with an asterisk.

available, studies of fungal infections indicate that posaconazole resistance occurs mainly by a mechanism involving mutation of the *cyp51* gene (23, 33, 35). Posaconazole appears to be less susceptible to the efflux pumps that confer resistance to some other azoles (7, 25, 35). Mapping mutations in *cyp51* genes in clinical posaconazole-resistant isolates on the CYP51-posaconazole structure (9) points to the mouth of the posaconazole binding tunnel as a mutation hot spot. Mutations of G54, P216, and M220 in clinical isolates of *Aspergillus fumigatus* (10, 12, 13, 23, 27, 32) (corresponding to G49, P210, and F214, respectively, in *T. cruzi* CYP51 [$CYP51_{Tc}$]) and of A61 (46) and P230 (25) in clinical isolates of *Candida albicans* (I45 and P210, respectively, in $CYP51_{Tc}$) map directly to the tunnel mouth, where amino acids interact with the dangling long substituent tail of posaconazole extending into the tunnel (9). Mutations of G54 in *A. fumigatus* to arginine or tryptophan associate with moderate and high levels of resistance, respectively, and confer cross-resistance between itraconazole and posaconazole (27). Mutations of M220 confer cross-resistance to all azole drugs tested, including itraconazole, voriconazole, ravuconazole, and posaconazole (30, 39), and therefore may interfere with the entry of the drugs. In accordance with this assumption, posaconazole is reported to induce resistance to all azole drugs in *Candida parapsilosis in vitro* (35). The alarming perspective emerging from antifungal therapy efforts must be taken into consideration when designing antichagasic drugs targeting $CYP51_{Tc}$. While antifungal azoles do show promise, the less than 30% sequence identity between fungal and protozoan CYP51 targets suggests that a more direct approach may be a better route toward developing novel potent therapeutic CYP51 inhibitors.

Using clues from our previous work on CYP51 from *Mycobacterium tuberculosis* ($CYP51_{Mt}$), we focused on rationally designed nonazole inhibitors of $CYP51_{Tc}$. These inhibitors were based on an experimental hit obtained from screening a small-molecule-compound library against $CYP51_{Mt}$ (36). Analysis of the X-ray structure revealed that the *N*-[4-pyridyl]-formamide scaffold group (Fig. 1A, highlighted in gray) binds in the CYP51 active site via conserved residues and the heme prosthetic group. Structural characterization confirmed that these interactions in the complexes were preserved between $CYP51_{Mt}$ and five different compounds (8, 36), suggesting that this scaffold could be used efficiently instead of the azole or triazole groups to target a variety of chemotypes to the CYP51 active site. Based on the similarity of the chemical structures, the expanded-spectrum compound LP10 (Fig. 1B) was selected for its nanomolar binding affinity to $CYP51_{Tc}$ and its potent efficacy against *T. cruzi* in mammalian cells (8). As the pyridyl group of LP10 presumably coordinates to the heme iron, the indole substituent may fill the space occupied by the 2,4-difluorophenyl ring of fluconazole or posaconazole in their structurally characterized complexes with CYP51 (9).

In the present work, we evaluated the efficacy of LP10 in an animal model of acute Chagas' disease. The curative effect of LP10 *in vivo* was comparable to that of the protease inhibitor K777, an antichagasic drug in preclinical development, used as a positive control (15, 16). Electron microscopy and gas chromatography-mass spectrometry (GC-MS) analysis demonstrated that treatment with LP10 disrupted cell membranes in *T. cruzi* amastigotes and altered sterol composition via accumulation of the C-14-methylated precursors lanosterol and 24-methylene-dihydrolanosterol (eburicol). There was concomitant reduction of 14-desmethylated fecosterol and episterol. LP10-induced alterations are consistent with the inhibition of *T. cruzi* CYP51.

MATERIALS AND METHODS

Reagents. Recombinant $CYP51_{Tc}$ was prepared as described elsewhere (8). Compound LP10 {α-[(4-methylcyclohexyl)carbonyl amino]-*N*-4-pyridinyl-1H-indole-3-propanamide} was purchased from ChemDiv (C155-0123) (San Diego, CA). Posaconazole (Noxafil; Schering-Plough) was purchased from a pharmacy. The active ingredient was purified by organic solvent extraction and separated by flash chromatography using an Isolera flash purification system (Biotage). All starting materials and solvents were commercially available high-pressure liquid chromatography (HPLC)-grade chemicals and were used without further purification. Briefly, 6.0 ml of posaconazole suspension was added to a 1-liter separating funnel, diluted with 150 ml of water, and extracted three times with 250 ml ethyl acetate. To trace posaconazole, each extraction step was monitored by thin-layer chromatography (TLC) using silica gel plates (Al-Sil, 250 μm, 60 Å; Whatman) with 5% methanol in dichloromethane as a mobile phase. The organic layers from three extractions were combined and evaporated to dryness. The solid white material was then purified by flash chromatography using a 40-g silica cartridge (Redi-Sep). Posaconazole was eluted from the column with a 1% to 10% gradient of methanol in dichloromethane over 10 column volumes to yield 247.7 mg of final product (88.5% recovery). The identity of the product was confirmed by liquid chromatography-mass spectrometry (LC-MS) analysis performed with a Waters Alliance HPLC system (Waters 2695 separations module and Waters 2487 dual absorbance detector).

Spectroscopic binding assay. To minimize experimental error, binding assays were performed by spectrophotometric titration with 3 ml of 50 mM Tris-HCl (pH 7.5) containing 10% glycerol, using a Cary UV-visible (UV-vis) scanning spectrophotometer (Varian). The $CYP51_{Tc}$ concentration was 0.1 μM. A stock solution of LP10 was prepared in dimethyl sulfoxide (DMSO) at 0.02 μM. Titrations were conducted using a 3.5-ml 6Q quartz cuvette with a path length of 1 cm, and the inhibitor was added in 0.3-μl aliquots by use of a 0.5-μl graduated capillary tube. The same amounts of DMSO alone were added to a reference cuvette, followed by recording of difference spectra. To determine the K_D (dissociation constant) values, titration data points were fitted to quadratic hyperbola using GraphPad PRISM software (GraphPad Software Inc.), as follows: $A_{obs} = (A_{max}/2 \times E_t)\{(S + E_t + K_D) - [(S + E_t + K_D)^2 - 4 \times S \times E_t]^{0.5}\}$, where A_{obs} is the absorption shift determined at any ligand concentration, A_{max} is the maximal absorption shift obtained at saturation, K_D is the dissociation constant for the inhibitor-enzyme complex, E_t is the total enzyme concentration used, and S is the ligand concentration.

Docking of LP10 in the $CYP51_{Tc}$ binding site. Molecular docking was performed using the crystal structure of CYP51 (Protein Data Bank [PDB] code 2WUZ) (9) to predict the binding modes of LP10. All docking calculations were carried out using Glide, with the OPLS2005 force field (21). In order to account for protein flexibility, the induced-fit docking protocol was utilized (40). The *S*

TABLE 1. Efficacy of LP10 in an animal model of Chagas' disease, as determined by the number of mice testing negative or positive for the presence of *T. cruzi*

Treatment group	Total no. of mice tested	No. of mice testing negative (N) or positive (P) by:													
		Hemoculture		PCR		Histology									
						Heart		Skeletal muscle		Liver		Spleen		Colon	
		N	P	N	P	N	P	N	P	N	P	N	P	N	P
Untreated	5	0	5	1	4	2	3	1	4	5	0	5	0	4[a]	0
K777	5	4	1	4	1	5	0	4	1	5	0	5	0	5	0
LP10	5	2[b]	2	4	1	4	1	3	2	5	0	5	0	5	0

[a] One mouse was not tested.
[b] One of five hemocultures of LP10-treated mice was discarded due to contamination.

and *R* stereoisomers of LP10 were prepared by the Ligprep module. The rigid receptor grid was first prepared from the crystal structure using the Protein Preparation Wizard module. The receptor then underwent constrained minimization, followed by docking in extra precision (XP) mode (22), in which the van der Waals radii of both protein and ligand were softened by a factor of 0.5 and the Fe^{3+} of the heme group was specified for metal constraint. Up to 20 poses for each isomer were subsequently processed to generate their corresponding induced-fit protein receptors. By use of PRIME, the side-chain conformations of residues within 5 Å from the docked molecule were predicted before these residues and the ligand were further optimized (47). Lastly, only those relaxed complexes within 30 kcal/mol of the lowest-energy complex were redocked and scored in XP mode.

Animal treatment. Three groups of five 7- to 8-week-old female C3H mice (Jax), mean weight of 17.5 to 18.0 g, were infected intraperitoneally (i.p.) with 10^6 tissue culture trypomastigotes of CA-I/72 *T. cruzi*. A control group of animals was left untreated, while treatment of the two other groups started 24 h postinfection. Animals in the experimental group were treated with an i.p. dose of 40 mg LP10/kg of body weight, resuspended in 100 μl solvent (60% DMSO–40% double-distilled water [ddH_2O]), twice a day (BID) for 30 days. Animals in the second control group were treated with K777, an inhibitor of the *T. cruzi* cysteine protease cruzain (also known as cruzipain or GP57/51), at an i.p. dose of 50 mg/kg in 100 μl solvent (30% DMSO-70% ddH_2O) BID for 30 days. Animals were sacrificed 6 months postinfection for evaluation.

Evaluation of treatment efficacy. To evaluate treatment efficacy and assess animal cure, we used conventional histology, hemoculture, and PCR. Selected tissues were dissected for histopathological observation (i.e., heart, skeletal muscle, liver, spleen, and colon), fixed in paraformaldehyde, and stained with hematoxylin-eosin. Blood samples (~150 μl) were obtained by heart puncture prior to necropsy. PCR of blood samples (50 μl) was performed as described elsewhere (1). Hemocultures were initiated with blood cell pellets (75 to 80 μl), resuspended in 5 ml of BHT medium (17), and maintained for up to 90 days. Cultures were observed weekly by phase-contrast microscopy for the presence of *T. cruzi* epimastigotes. Fifty percent of the BHT medium was replaced every 15 days. Results are summarized in Table 1.

Preparation of amastigotes and epimastigotes for lipid analyses. Amastigotes of the *T. cruzi* CA-I/72 cloned stock were cultured in bovine embryo skeletal muscle (BESM) cells maintained in RPMI 1640 medium supplemented with 5% heat-inactivated fetal calf serum in a 5% CO_2 atmosphere at 37°C. For large-scale production of amastigotes, confluent monolayers of BESM cells in 75-cm^2 tissue culture flasks (two flasks per treatment) were infected with 4×10^7 parasites/ml for 24 h. The medium was then replaced with LP10 (5 μM), posaconazole (5 μM), or DMSO alone. Noninfected BESM cells were used as a negative control. Under these growing conditions, some intracellular parasites were transforming to trypomastigotes at 72 h postinfection. Thirty-six hours posttreatment, cells were scraped and pooled as appropriate, washed twice with 10 ml phosphate-buffered saline (PBS), pH 7.4, transferred in this buffer to glass tubes, and centrifuged at 1,500 rpm for 10 min. The pellet was finally resuspended in 2 ml of chloroform-methanol (2:1 ratio) and dried under a stream of nitrogen gas.

Epimastigotes in log phase were cultured axenically in rich BHT medium containing fetal bovine serum and brain heart infusion, both rich in lipids, including cholesterol (5, 17). Epimastigotes were treated with 5 μM LP10 or posaconazole for 72 h. Untreated epimastigotes were used as a control. Parasites were centrifuged at 2,000 rpm for 10 min, washed twice with PBS, and processed further as described above for amastigotes.

Sterol extraction. Total cellular lipids were first extracted by treating the dry cell pellets with chloroform for 24 h at room temperature, washing the chloroform extract with water, and reserving the organic phase that was subsequently dried under a stream of nitrogen gas. Sterols were partitioned by resuspension three times in 2 ml chloroform-methanol (9:1 ratio). The combined organic phase was dried three times by being dissolved in acetonitrile followed by evaporation under a stream of nitrogen gas.

Analysis of sterol composition. Our analysis of sterols from amastigotes and epimastigotes was expedited by the use of GC-MS, wherein the components of a complex sterol mixture were separated and subsequently analyzed by mass spectrometry. Extracted sterols were derivatized with *N*,*N*-bis(trimethylsilyl)-2,2,2-trifluoroacetamide (BSTFA) (Pierce) and analyzed by GC-MS as their trimethylsilyl (TMS) derivatives. For this procedure, the dried sterol residue from the previous step was mixed with 75 μl of BSTFA (5 mg/ml in dimethylformamide), incubated for 2 h in a sealed vial, and directly injected into an HP5790 gas chromatography system equipped with a mass selective detector (MSD). Chromatographic separation of sterols in the GC system was carried out using a DB5-MS column (30 m, inside diameter [i.d.] of 0.25 mm, 0.33-μm film thickness). The column temperature was kept at 200°C for 1 min, and then the temperature was increased to 300°C at a rate of 15°C/min and finally maintained at 300°C for 20 min. The temperatures of the injector GC inlet and the MSD were 250°C and 300°C, respectively.

Sterol-TMS derivatives produce characteristic quasimolecular ions ($[M-90]^{\bullet+}$ and $[M+73]^{\bullet+}$, where M is the molecular mass of the compound minus an electron), from which the nominal molecular masses were calculated. The signature molecular ions and fragmentation patterns, used in conjunction with standard samples, allowed us to assign identities of components of interest (see Table S1 in the supplemental material). Squalene, lanosterol, and ergosterol, purchased from Sigma-Aldrich, were used as standards. Cholesterol served as an additional internal standard.

Ultrastructural analysis by electron microscopy. BESM cells were infected with *T. cruzi* and treated with LP10 (10 μm) or posaconazole (0.25 μM) for 48 h

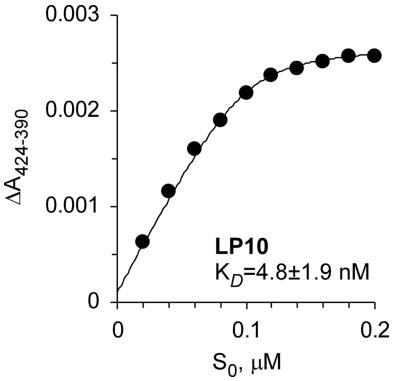

FIG. 2. Binding of LP10 to $CYP51_{Tc}$. The concentration dependence of LP10 binding was determined by titration of $CYP51_{Tc}$ (0.1 μM) with increasing concentrations of the inhibitor. The binding absorption curve plateaus at a 1:1 protein-inhibitor ratio.

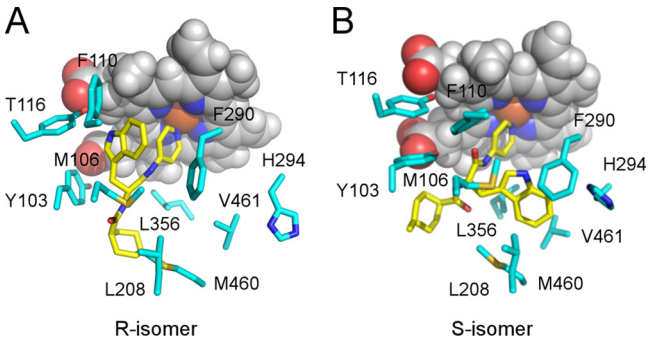

FIG. 3. Induced-fit docking of LP10 in the active site of $CYP51_{Tc}$. The different binding modes predicted for the *R* (A) and *S* (B) stereoisomers of LP10 are shown. LP10 is highlighted in yellow, and protein side chains within 5 Å are in cyan. Heme is shown by van der Waals spheres, with carbon in gray, oxygen in red, nitrogen in blue, and iron in orange.

and 72 h. Untreated controls were similarly infected and processed. Samples were fixed overnight at 4°C by immersion in 0.1 M sodium cacodylate buffer, pH 7.4, supplemented with 2.5% glutaraldehyde. The samples were then postfixed with 2% osmium tetroxide plus 1% potassium ferrocyanide in 0.1 M sodium cacodylate buffer, pH 7.4, dehydrated with an ascending series of ethyl alcohol and propylene oxide, and finally embedded in a medium mixture of EMbed 812 (Electron Microscopy Sciences, Fort Washington, PA). Thin sections (75 to 85 nm) were cut with a diamond knife, mounted on 200-mesh copper grids, and counterstained with 2% aqueous uranyl acetate followed by Reynold's lead citrate. *T. cruzi* thin sections were examined using an FEI Tecnai T12 transmission electron microscope (TEM).

RESULTS AND DISCUSSION

Binding to the $CYP51_{Tc}$ target. The binding affinity of LP10 to $CYP51_{Tc}$ was reexamined using a spectroscopic UV-vis assay. The assay utilizes the property of P450 enzymes to shift the ferric heme iron Soret band following replacement of a water ligand with the aromatic nitrogen of the pyridinyl group. The increased volume of the titration mix (3 ml) and the use of

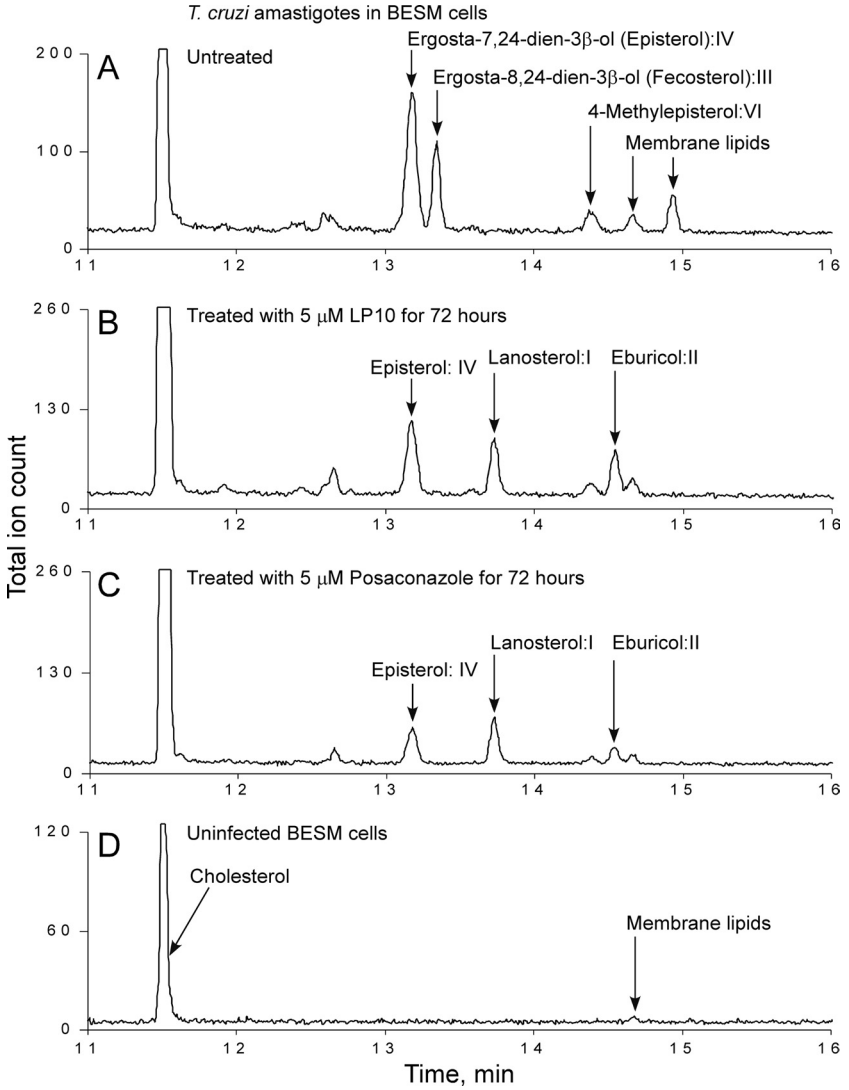

FIG. 4. Analysis of sterol composition in amastigotes. GC-MS traces are shown for amastigotes isolated from infected BESM cells either untreated (A) or treated with 5 μM LP10 (B) or 5 μM posaconazole (C) and for extract from noninfected BESM cells (D). All sterols identified are labeled. Unidentified lipids of nonsterol origin are labeled as membrane lipids.

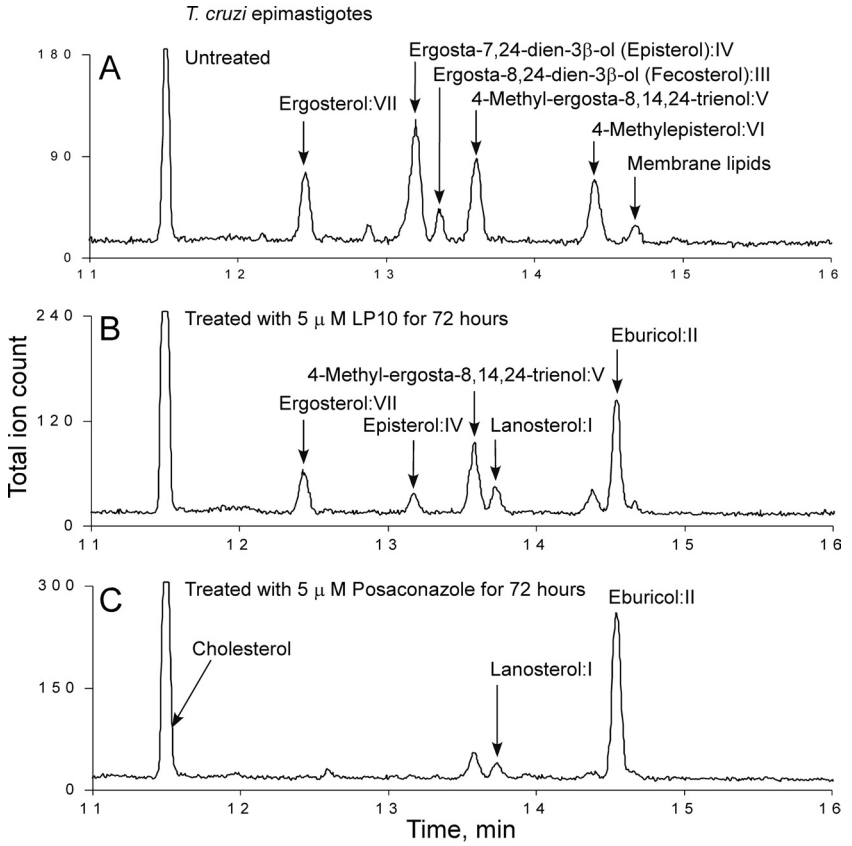

FIG. 5. Analysis of sterol composition in epimastigotes. GC-MS traces are shown for epimastigotes isolated from untreated parasites (A) or parasites treated with 5 μM LP10 (B) or 5 μM posaconazole (C). All sterols identified are labeled. Unidentified lipids of nonsterol origin are labeled as membrane lipids.

0.5-μl graduated capillary tubes for adding an inhibitor improved the signal-to-noise ratio and allowed the use of protein concentrations as low as 0.1 μM. An upper limit for the K_D values estimated under these conditions was 4.8 nM, an order of magnitude lower than that previously reported (8). However, as the binding curve still plateaus at a protein-inhibitor ratio of 1:1 (Fig. 2), true dissociation constants must be lower, perhaps in the picomolar range. Thus, the sensitivity of UV-vis spectroscopy sets a lower limit for accurate K_D determination at ~0.1 μM. Compounds with higher binding affinities cannot be discriminated by the standard UV-vis assay.

Computational docking of the *S* and *R* stereoisomers of LP10 predicted different modes of binding to $CYP51_{Tc}$ (Fig. 3). The binding affinities of both isomers to $CYP51_{Tc}$ are predicted to be similar, as the Glide XP docking scores for the *S* and *R* isomers are, respectively, −8.9 and −9.3. These calculations predict that the indole ring of the *R* isomer will fill the space occupied by the 2,4-difluorophenyl ring of fluconazole or posaconazole in its structurally characterized complex with CYP51 (9). Stacking interactions with the aromatic residues Y103, Y116, and F100 and the heme macrocycle contribute to this binding mode (Fig. 3A). The indole ring of the *S* isomer is predicted to bind in the hydrophobic pocket formed by the residues M106, L208, F290, H294, L356, M460, and V461 (Fig. 3B). As shown in prior work, the interactions of the indole ring are extremely important for the potency of LP10, as related compounds lacking this feature have their affinities reduced by 3 orders of magnitude (8). Definitive determination of the LP10 chirality and the binding mode awaits determination of the X-ray structure of the $CYP51_{Tc}$-LP10 complex.

Efficacy of LP10 in a mouse model of Chagas' disease. Because LP10 bound $CYP51_{Tc}$ tightly, was lethal for *T. cruzi* in mammalian cells, and showed no toxicity to host cells at curative concentrations (8), it was tested in a mouse model of acute Chagas' disease. Doses of 40 mg LP10/kg were given 24 h postinfection BID for 30 days to five female mice infected with *T. cruzi*. In the two control groups, animals were either left untreated or treated with the protease inhibitor K777 (15, 16). By day 12 postinfection, all five animals in the untreated control group had enlarged abdomens due to ascites, indicative of heart failure, and weakness in their hind legs due to muscle infection and atrophy. Mice in the K777-treated control group appeared normal and agile, with normal muscles in their hind legs and no gross ascites. The results of treatment with LP10 were similar to those obtained with K777. Mean weights at the end of the experiment were 32.2 g for untreated controls, 29.0 g for K777-treated mice, and 30.5 g for LP10-treated mice. Histopathological studies of the LP10-treated group showed normal major organ tissues. While LP10 treatment clearly spared mice the clinical manifestations of acute Chagas' disease, we also stringently tested for the presence of any residual parasites. PCR was negative in 4/5 LP10-treated mice, and

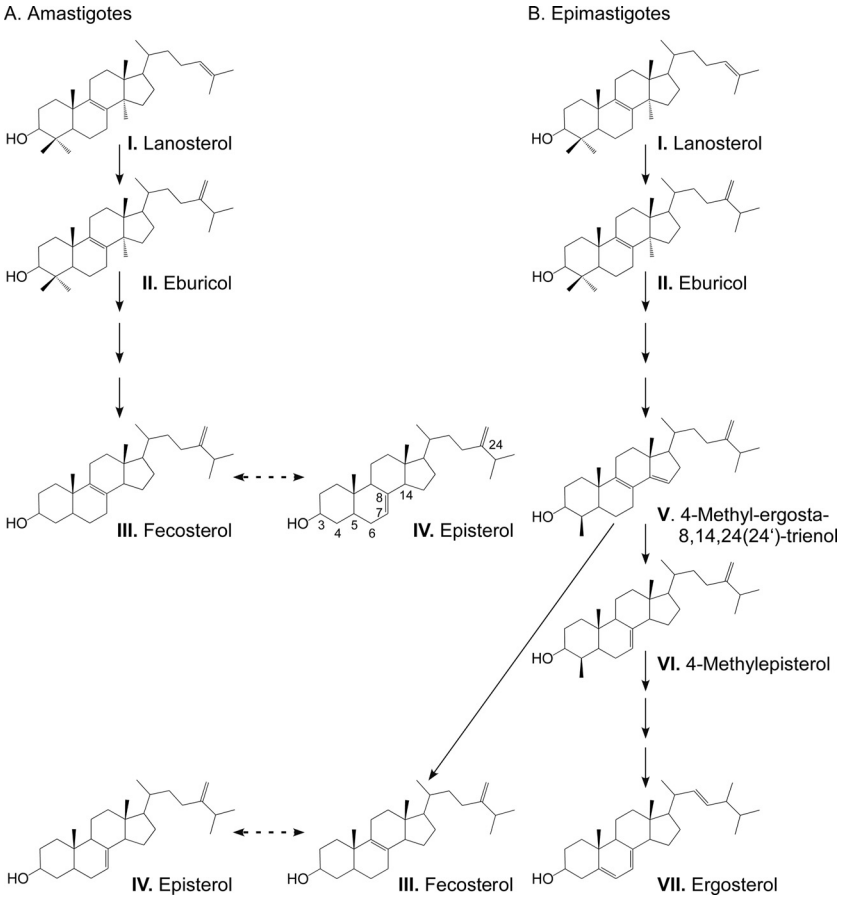

FIG. 6. Sterol biosynthesis in amastigotes and epimastigotes. Partial sterol biosynthesis pathways, which include all sterols identified by GC-MS analyses in this work, are shown for amastigotes (A) and epimastigotes (B). I, lanosterol (4,4,14-trimethylcholesta-8,24-dien-3ß-ol); II, eburicol (24-methylenedihydrolanosterol); III, fecosterol [ergosta-8,24(24′)-dien-3ß-ol]; IV, episterol [ergosta-7,24(24′)-dien-3ß-ol]; V, 4-methyl-ergosta-8,14,24(24′)-trienol; VI, 4-methylepisterol [4-methylcholesta-7,24(24′)-dien-3ß-ol]; VII, ergosterol (ergosta-5,7,22-trien-3ß-ol).

parasites could not even be detected by amplification in 2/4 hemocultures (one of five hemocultures of LP10-treated mice was discarded due to contamination) (Table 1).

Inhibition of 14α-demethylation by LP10. To confirm that LP10 targets $CYP51_{Tc}$, we analyzed sterol composition in *T. cruzi* extracts from intracellular amastigotes cultured in BESM cells and from axenically cultured insect epimastigotes. Cultures were either untreated or treated with LP10 or posaconazole. Examples of GC-MS traces are shown for amastigotes (Fig. 4) and epimastigotes (Fig. 5). Untreated, *T. cruzi*-infected BESM cells (Fig. 4A) were used as a positive control, and noninfected BESM cells (Fig. 4D) were used as an additional control for comparison with amastigote-infected cells treated with 5 μM LP10 (Fig. 4B) or posaconazole (Fig. 4C) for 72 h. Similarly, epimastigotes were either untreated (Fig. 5A) or treated with LP10 (Fig. 5B) or posaconazole (Fig. 5C).

The sterol identities were assigned based on relative chromatographic behaviors as well as the characteristic molecular masses and fragmentation patterns (Fig. 4 and 5; also see Fig. S1 to S3 and Table S2 in the supplemental material). Our assignments are similar to those reported elsewhere (26, 41). Identified sterols are as follows: I, lanosterol (4,4,14-trimethylcholesta-8,24-dien-3β-ol); II, eburicol (24-methylenedihydrolanosterol); III, fecosterol [ergosta-8,24(24′)-dien-3β-ol]; IV, episterol [ergosta-7,24(24′)-dien-3β-ol]; V, 4-methyl-ergosta-8,14,24(24′)-trienol; VI, 4-methylepisterol [4-methylcholesta-7,24(24′)-dien-3β-ol]; and VII, ergosterol (ergosta-5,7,22-trien-3β-ol). Fecosterol and its Δ8-Δ7 isomer episterol were identified as principal sterols in the untreated amastigotes, where no Δ5 sterols or ergosterol was detected. This observation is consistent with results reported elsewhere (26, 43). The untreated epimastigotes revealed a pool of sterols richer than that found with amastigotes, consisting of a mix of ergosterol, episterol, fecosterol, and 14-desmethyl intermediates 4-methyl-ergosta-8,14,24(24′)-trienol and 4-methylepisterol. Exogenous cholesterol was present in both epimastigote and amastigote samples (Fig. 4 and 5).

Both LP10 and posaconazole induced similar changes in sterol composition in *T. cruzi* amastigotes and epimastigotes. In amastigotes, treatment with either of the two inhibitors at 5 μM for 72 h resulted in the complete depletion of fecosterol and a significant reduction in episterol content, with concomitant accumulation of lanosterol and eburicol precursors (Fig. 4B and C). Similar effects were observed in epimastigotes. Although the pool of the 14-demethylated sterols in the membranes of untreated epimastigotes is more diversified than that

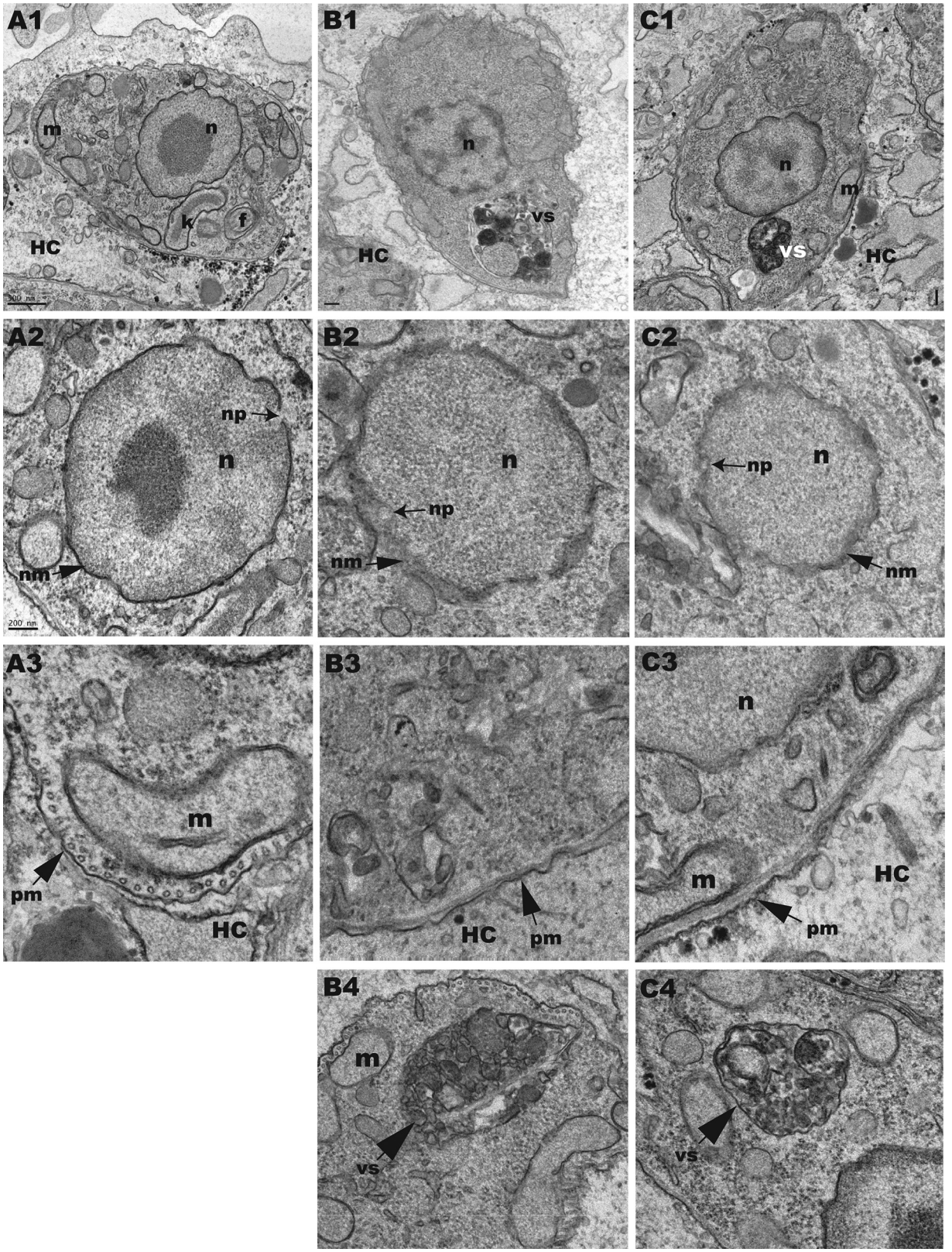

FIG. 7. Ultrastructural alterations in *T. cruzi* intracellular amastigotes. Forty-eight hours of treatment with 10 μM LP10 (B1 to B4) or 0.25 μM posaconazole (C1 to C4) induced ultrastructural alterations in *T. cruzi* intracellular amastigotes. (A1) Untreated amastigote cell. (A2) Untreated amastigote nucleus. (A3) Untreated amastigote plasma membrane. (B1) LP10-treated amastigote cell. (B2) LP10-induced alterations in the amastigote nuclear membrane. (B3) LP10-induced alterations in the amastigote plasma membrane. (B4) Vesicular structure induced in an LP10-treated amastigote. (C1) Posaconazole-treated amastigote cell. (C2) Posaconazole-induced alterations in the amastigote nuclear membrane. (C3) Posaconazole-induced alterations in the amastigote plasma membrane. (C4) Vesicular structure induced in a posaconazole-treated amastigote. HC, host cell; n, parasite nucleus; nm, nuclear membrane; np, nuclear pore; m, parasite mitochondria; k, parasite kinetoplast; f, flagellum/flagellar pocket; pm, parasite plasma membrane; vs, vesicular structure.

in amastigotes (Fig. 5A), they virtually disappeared upon treatment with posaconazole (Fig. 5C). Residual amounts of ergosterol were detected in the LP10-treated epimastigotes (Fig. 5B). These overall results indicate that LP10, similarly to posaconazole, targets $CYP51_{Tc}$ and blocks sterol biosynthesis efficiently in both *T. cruzi* amastigotes and epimastigotes.

T. cruzi amastigote and epimastigote sterol biosynthetic pathways were partially reconstructed from the sterols identified experimentally (Fig. 6). The pathway appears straightforward in amastigotes (Fig. 6A), while branching is required to explain the more complex composition of the identified sterols in epimastigotes (Fig. 6B).

Alterations in *T. cruzi* amastigote ultrastructure. A 48-h treatment with CYP51 inhibitors induced major changes in the ultrastructure of amastigote cells, including blebbing of the cell membrane, swelling of the nuclear membrane, and appearance of large autophagic vesicles (Fig. 7). Finally, a 72-h treatment with LP10 or posaconazole caused severe abnormalities in the nuclear envelope and nuclear DNA and cell death. In contrast, epimastigotes treated with either LP10 or posaconazole at similar concentrations continued to divide normally, and no morphological changes were observed by electron microscopy after 72 h, despite the fact that 14-desmethyl sterols were largely depleted at that time. The different susceptibilities of amastigotes and epimastigotes to CYP51 inhibitors, though well documented in the literature (26, 41), are still unclear.

In summary, a search for structurally and synthetically simpler CYP51 inhibitors led us to identify the nonazole inhibitor LP10, which shows potent antichagasic activity in a mouse model of acute *T. cruzi* infection. The 60% cure rate obtained with LP10 compares favorably with the previously reported 50 to 100% cure rate obtained with posaconazole in experimental acute infections (2). Analyses of sterol composition confirmed that LP10 inhibits the 14α-demethylation step in the sterol biosynthetic pathway in *T. cruzi*, leading to the accumulation of lanosterol and eburicol precursors and to the decline of 14-desmethyl sterols in both proliferative stages of the parasite. The clinically relevant intracellular-amastigote stage was more sensitive to treatment with CYP51 inhibitors than the insect vector epimastigote form. Blockage of the 14α-demethylation step in amastigotes by both LP10 and posaconazole initiated alterations in cell membranes that culminated in severe ultrastructural and morphological changes and cell death by 72 h posttreatment. LP10 will serve as a starting point for medicinal-chemistry efforts to optimize drug-like properties and develop compounds specifically tailored to inhibit the *T. cruzi* sterol 14α-demethylase.

ACKNOWLEDGMENTS

We thank Potter Wickware for critical reading of the manuscript and Clifford Bryant for valuable contributions.

This work was supported by NIH RO1 grants GM078553 (to L.M.P.) and GM086602 (to M.P.J.) and by the Sandler Foundation. J.B.J. was supported by grant AI074824 to Paul Ortiz de Montellano.

M.P.J. is a consultant to Schrodinger, LLC.

REFERENCES

1. **Avila, H. A., J. B. Pereira, O. Thiemann, E. De Paiva, W. DeGrave, C. M. Morel, and L. Simpson.** 1993. Detection of *Trypanosoma cruzi* in blood specimens of chronic chagasic patients by polymerase chain reaction amplification of kinetoplast minicircle DNA: comparison with serology and xenodiagnosis. J. Clin. Microbiol. **31:**2421–2426.
2. **Buckner, F.** 2008. Sterol 14-demethylase inhibitors for *Trypanosoma cruzi* infections, p. 61–80. *In* H. K. Majumder (ed.), Drug targets in kinetoplastid parasites, vol. 625. Springer, New York, NY.
3. **Buckner, F. S., B. M. Joubert, S. M. Boyle, R. T. Eastman, C. L. Verlinde, and S. P. Matsuda.** 2003. Cloning and analysis of *Trypanosoma cruzi* lanosterol 14alpha-demethylase. Mol. Biochem. Parasitol. **132:**75–81.
4. **Buckner, F. S., A. J. Wilson, T. C. White, and W. C. Van Voorhis.** 1998. Induction of resistance to azole drugs in *Trypanosoma cruzi*. Antimicrob. Agents Chemother. **42:**3245–3250.
5. **Cazzulo, J. J., B. M. Franke de Cazzulo, J. C. Engel, and J. J. Cannata.** 1985. End products and enzyme levels of aerobic glucose fermentation in trypanosomatids. Mol. Biochem. Parasitol. **16:**329–343.
6. **Chagas, C.** 1909. Nova trypanosomiase humana. Gac. Med. Bahia **40:**433–440.
7. **Chau, A. S., C. A. Mendrick, F. J. Sabatelli, D. Loebenberg, and P. M. McNicholas.** 2004. Application of real-time quantitative PCR to molecular analysis of *Candida albicans* strains exhibiting reduced susceptibility to azoles. Antimicrob. Agents Chemother. **48:**2124–2131.
8. **Chen, C.-K., P. S. Doyle, L. V. Yermalitskaya, Z. B. Mackey, K. K. H. Ang, J. H. McKerrow, and L. M. Podust.** 2009. *Trypanosoma cruzi* CYP51 inhibitor derived from a *Mycobacterium tuberculosis* screen hit. PLoS Negl. Trop. Dis. **3:**e372.
9. **Chen, C.-K., S. S. F. Leung, C. Guilbert, M. P. Jacobson, J. H. McKerrow, and L. M. Podust.** 2010. Structural characterization of CYP51 from *Trypanosoma cruzi* and *Trypanosoma brucei* bound to the antifungal drugs posaconazole and fluconazole. PLoS Negl. Trop. Dis. **4:**e651.
10. **Chen, J., H. Li, R. Li, D. Bu, and Z. Wan.** 2005. Mutations in the cyp51A gene and susceptibility to itraconazole in *Aspergillus fumigatus* serially isolated from a patient with lung aspergilloma. J. Antimicrob. Chemother. **55:**31–37.
11. **Croft, S. L., M. P. Barrett, and J. A. Urbina.** 2005. Chemotherapy of trypanosomiases and leishmaniasis. Trends Parasitol. **21:**508–512.
12. **da Silva Ferreira, M. E., J. L. Capellaro, E. dos Reis Marques, I. Malavazi, D. Perlin, S. Park, J. B. Anderson, A. L. Colombo, B. A. Arthington-Skaggs, M. H. Goldman, and G. H. Goldman.** 2004. In vitro evolution of itraconazole resistance in *Aspergillus fumigatus* involves multiple mechanisms of resistance. Antimicrob. Agents Chemother. **48:**4405–4413.
13. **Diaz-Guerra, T. M., E. Mellado, M. Cuenca-Estrella, and J. L. Rodriguez-Tudela.** 2003. A point mutation in the 14alpha-sterol demethylase gene cyp51A contributes to itraconazole resistance in *Aspergillus fumigatus*. Antimicrob. Agents Chemother. **47:**1120–1124.
14. **Doyle, P. S., M. Sajid, T. O'Brien, K. Dubois, J. C. Engel, Z. B. Mackey, and S. Reed.** 2008. Drugs targeting parasite lysosomes. Curr. Pharm. Des. **14:**889–900.
15. **Doyle, P. S., Y. M. Zhou, J. C. Engel, and J. H. McKerrow.** 2007. A cysteine protease inhibitor cures Chagas' disease in an immunodeficient-mouse model of infection. Antimicrob. Agents Chemother. **51:**3932–3939.
16. **Engel, J. C., P. S. Doyle, I. Hsieh, and J. H. McKerrow.** 1998. Cysteine protease inhibitors cure an experimental *Trypanosoma cruzi* infection. J. Exp. Med. **188:**725–734.
17. **Engel, J. C., B. M. Franke de Cazzulo, A. O. Stoppani, J. J. Cannata, and J. J. Cazzulo.** 1987. Aerobic glucose fermentation by *Trypanosoma cruzi* axenic culture amastigote-like forms during growth and differentiation to epimastigotes. Mol. Biochem. Parasitol. **26:**1–10.
18. **Ferraz, M. L., R. T. Gazzinelli, R. O. Alves, J. A. Urbina, and A. J. Romanha.** 2007. The anti-*Trypanosoma cruzi* activity of posaconazole in a murine model of acute Chagas' disease is less dependent on gamma interferon than that of benznidazole. Antimicrob. Agents Chemother. **51:**1359–1364.
19. **Fischer, R., J. Trzaskos, R. Magolda, S. Ko, C. Brosz, and B. Larsen.** 1991. Lanosterol 14 alpha-methyl demethylase. Isolation and characterization of the third metabolically generated oxidative demethylation intermediate. J. Biol. Chem. **266:**6124–6132.
20. **Fischer, R. T., S. H. Stam, P. R. Johnson, S. S. Ko, R. L. Magolda, J. L. Gaylor, and J. M. Trzaskos.** 1989. Mechanistic studies of lanosterol 14 alpha-methyl demethylase: substrate requirements for the component reactions catalyzed by a single cytochrome P-450 isozyme. J. Lipid Res. **30:**1621–1632.
21. **Friesner, R. A., J. L. Banks, R. B. Murphy, T. A. Halgren, J. J. Klicic, D. T. Mainz, M. P. Repasky, E. H. Knoll, M. Shelley, J. K. Perry, D. E. Shaw, P. Francis, and P. S. Shenkin.** 2004. Glide: a new approach for rapid, accurate docking and scoring. 1. Method and assessment of docking accuracy. J. Med. Chem. **47:**1739–1749.
22. **Friesner, R. A., R. B. Murphy, M. P. Repasky, L. L. Frye, J. R. Greenwood, T. A. Halgren, P. C. Sanschagrin, and D. T. Mainz.** 2006. Extra precision glide: docking and scoring incorporating a model of hydrophobic enclosure for protein-ligand complexes. J. Med. Chem. **49:**6177–6196.
23. **Howard, S. J., D. Cerar, M. J. Anderson, A. Albarrag, M. C. Fisher, A. C. Pasqualotto, M. Laverdiere, M. C. Arendrup, D. S. Perlin, and D. W. Denning.** 2009. Frequency and evolution of azole resistance in *Aspergillus fumigatus* associated with treatment failure. Emerg. Infect. Dis. **15:**1068–1076.
24. **Hucke, O., M. H. Gelb, C. L. Verlinde, and F. S. Buckner.** 2005. The protein

farnesyltransferase inhibitor Tipifarnib as a new lead for the development of drugs against Chagas disease. J. Med. Chem. **48:**5415–5418.
25. **Li, X., N. Brown, A. S. Chau, J. L. Lopez-Ribot, M. T. Ruesga, G. Quindos, C. A. Mendrick, R. S. Hare, D. Loebenberg, B. DiDomenico, and P. M. McNicholas.** 2004. Changes in susceptibility to posaconazole in clinical isolates of *Candida albicans*. J. Antimicrob. Chemother. **53:**74–80.
26. **Liendo, A., G. Visbal, M. M. Piras, R. Piras, and J. A. Urbina.** 1999. Sterol composition and biosynthesis in *Trypanosoma cruzi* amastigotes. Mol. Biochem. Parasitol. **104:**81–91.
27. **Mann, P. A., R. M. Parmegiani, S. Q. Wei, C. A. Mendrick, X. Li, D. Loebenberg, B. DiDomenico, R. S. Hare, S. S. Walker, and P. M. McNicholas.** 2003. Mutations in *Aspergillus fumigatus* resulting in reduced susceptibility to posaconazole appear to be restricted to a single amino acid in the cytochrome P450 14alpha-demethylase. Antimicrob. Agents Chemother. **47:** 577–581.
28. **McCabe, R.** 1988. Failure of ketoconazole to cure chronic murine Chagas' disease. J. Infect. Dis. **158:**1408–1409.
29. **McKerrow, J. H., P. J. Rosenthal, R. Swenerton, and P. Doyle.** 2008. Development of protease inhibitors for protozoan infections. Curr. Opin. Infect. Dis. **21:**668–672.
30. **Mellado, E., G. Garcia-Effron, L. Alcazar-Fuoli, M. Cuenca-Estrella, and J. L. Rodriguez-Tudela.** 2004. Substitutions at methionine 220 in the 14alpha-sterol demethylase (Cyp51A) of *Aspergillus fumigatus* are responsible for resistance in vitro to azole antifungal drugs. Antimicrob. Agents Chemother. **48:**2747–2750.
31. **Morris, M. I.** 2009. Posaconazole: a new oral antifungal agent with an expanded spectrum of activity. Am. J. Health Syst. Pharm. **66:**225–236.
32. **Nascimento, A. M., G. H. Goldman, S. Park, S. A. Marras, G. Delmas, U. Oza, K. Lolans, M. N. Dudley, P. A. Mann, and D. S. Perlin.** 2003. Multiple resistance mechanisms among *Aspergillus fumigatus* mutants with high-level resistance to itraconazole. Antimicrob. Agents Chemother. **47:**1719–1726.
33. **Pfaller, M. A., D. J. Diekema, M. A. Ghannoum, J. H. Rex, B. D. Alexander, D. Andes, S. D. Brown, V. Chaturvedi, A. Espinel-Ingroff, C. L. Fowler, E. M. Johnson, C. C. Knapp, M. R. Motyl, L. Ostrosky-Zeichner, D. J. Sheehan, and T. J. Walsh.** 2009. Wild-type MIC distribution and epidemiological cutoff values for *Aspergillus fumigatus* and three triazoles as determined by the Clinical and Laboratory Standards Institute broth microdilution methods. J. Clin. Microbiol. **47:**3142–3146.
34. **Pinazo, M.-J., G. Espinosa, M. Gállego, P. L. López-Chejade, J. Urbina, and J. Gascón.** 2010. Treatment with posaconazole of a patient with systemic lupus erythematosus and Chagas disease. Am. J. Trop. Med. Hyg. **82:**583–587.
35. **Pinto e Silva, A. T., S. Costa-de-Oliveira, A. Silva-Dias, C. Pina-Vaz, and A. G. Rodrigues.** 2009. Dynamics of *in vitro* acquisition of resistance by *Candida parapsilosis* to different azoles. FEMS Yeast Res. **9:**626–633.
36. **Podust, L. M., J. P. von Kries, A. Nasser Eddine, Y. Kim, L. V. Yermalitskaya, R. Kuehne, H. Ouellet, T. Warrier, M. Altekoster, J.-S. Lee, J. Rademann, H. Oschkinat, S. H. E. Kaufmann, and M. R. Waterman.** 2007. Small-molecule scaffolds for CYP51 inhibitors identified by high-throughput screening and defined by X-ray crystallography. Antimicrob. Agents Chemother. **51:**3915–3923.
37. **Punukollu, G., R. M. Gowda, I. A. Khan, V. S. Navarro, and B. C. Vasavada.** 2007. Clinical aspects of the Chagas' heart disease. Int. J. Cardiol. **115:**279–283.
38. **Roberts, C. W., R. McLeod, D. W. Rice, M. Ginger, M. L. Chance, and L. J. Goad.** 2003. Fatty acid and sterol metabolism: potential antimicrobial targets in apicomplexan and trypanosomatid parasitic protozoa. Mol. Biochem. Parasitol. **126:**129–142.
39. **Rodriguez-Tudela, J. L., L. Alcazar-Fuoli, E. Mellado, A. Alastruey-Izquierdo, A. Monzon, and M. Cuenca-Estrella.** 2008. Epidemiological cutoffs and cross-resistance to azole drugs in *Aspergillus fumigatus*. Antimicrob. Agents Chemother. **52:**2468–2472.
40. **Sherman, W., T. Day, M. P. Jacobson, R. A. Friesner, and R. Farid.** 2006. Novel procedure for modeling ligand/receptor induced fit effects. J. Med. Chem. **49:**534–553.
41. **Taton, M., and A. Rahier.** 1991. Properties and structural requirements for substrate specificity of cytochrome P-450-dependent obtusifoliol 14alpha-demethylase from maize (Zea mays) seedlings. Biochem. J. **277:**483–492.
42. **Teixeira, A. R., N. Nitz, M. C. Guimaro, C. Gomes, and C. A. Santos-Buch.** 2006. Chagas disease. Postgrad. Med. J. **82:**788–798.
43. **Urbina, J. A., G. Payares, L. M. Contreras, A. Liendo, C. Sanoja, J. Molina, M. Piras, R. Piras, N. Perez, P. Wincker, and D. Loebenberg.** 1998. Antiproliferative effects and mechanism of action of SCH 56592 against *Trypanosoma* (*Schizotrypanum*) *cruzi*: *in vitro* and *in vivo* studies. Antimicrob. Agents Chemother. **42:**1771–1777.
44. **Urbina, J. A., G. Payares, J. Molina, C. Sanoja, A. Liendo, K. Lazardi, M. M. Piras, R. Piras, N. Perez, P. Wincker, and J. F. Ryley.** 1996. Cure of short- and long-term experimental Chagas' disease using D0870. Science **273:**969–971.
45. **Urbina, J. A., G. Payares, C. Sanoja, J. Molina, R. Lira, Z. Brener, and A. J. Romanha.** 2003. Parasitological cure of acute and chronic experimental Chagas disease using the long-acting experimental triazole TAK-187. Activity against drug-resistant *Trypanosoma cruzi* strains. Int. J. Antimicrob. Agents **21:**39–48.
46. **Xiao, L., V. Madison, A. S. Chau, D. Loebenberg, R. E. Palermo, and P. M. McNicholas.** 2004. Three-dimensional models of wild-type and mutated forms of cytochrome P450 14alpha-sterol demethylases from *Aspergillus fumigatus* and *Candida albicans* provide insights into posaconazole binding. Antimicrob. Agents Chemother. **48:**568–574.
47. **Zhu, K., M. R. Shirts, R. A. Friesner, and M. P. Jacobson.** 2007. Multiscale optimization of a truncated Newton minimization algorithm and application to proteins and protein-ligand complexes. J. Chem. Theory Comput. **3:**640–648.
48. **Zonios, D. I., and J. E. Bennett.** 2008. Update on azole antifungals. Semin. Respir. Crit. Care Med. **29:**198–210.